Development 130, 917-927

doi:10.1242/dev.00317

Differential function of RNCAM isoforms in precise target selection of olfactory sensory neurons

Mattias Alenius and Staffan Bohm*

Department of Molecular Biology, Umeå University, Umeå, S-901 87, Sweden
*Author for correpondence (e-mail: staffan.bohm@molbiol.umu.se)

Accepted 26 November 2002

SUMMARY

Olfactory sensory neurons (OSNs) are individually specified to express one odorant receptor (OR) gene among ~1000 different and project with precision to topographically defined convergence sites, the glomeruli, in the olfactory bulb. Although ORs partially determine the location of convergence sites, the mechanism ensuring that axons with different OR identities do not co-converge is unknown. RNCAM (OCAM, NCAM2) is assumed to regulate a broad zonal segregation of projections by virtue of being a homophilic cell adhesion molecule that is selectively expressed on axons terminating in a defined olfactory bulb region. We have identified NADPH diaphorase activity as being an independent marker for RNCAM-negative axons. Analyses of transgenic mice that ectopically express RNCAM in NADPH diaphorase-positive OSNs show that the postulated function of RNCAM in mediating zone-specific segregation of axons is unlikely. Instead, analyses of one OR-specific OSN subpopulation (P2) reveal that elevated RNCAM levels result in an increased number of P2 axons that incorrectly co-converge with axons of other OR identities. Both Gpi-anchored and transmembrane-bound RNCAM isoforms are localized on axons in the nerve layer, while the transmembrane-bound RNCAM is the predominant isoform on axon terminals within glomeruli. Overexpressing transmembrane-bound RNCAM results in co-convergence events close to the correct target glomeruli. By contrast, overexpression of Gpi-anchored RNCAM results in axons that can bypass the correct target before co-converging on glomeruli located at a distance. The phenotype specific for Gpi-anchored RNCAM is suppressed in mice overexpressing both isoforms, which suggests that two distinct RNCAM isoform-dependent activities influence segregation of OR-defined axon subclasses.

Key words: RNCAM, OCAM, NCAM2, apCAM, Fasciclin 2, Neural cell adhesion molecule, Splice variants, Olfactory, Sensory map, Gene expression, Odorant receptors, Axon guidance, Mouse, Glycosylphosphatidylinositol, Fasciculation

INTRODUCTION

Mouse olfactory sensory neurons (OSNs) are functionally specified to express one specific odorant receptor (OR) out of more than 1000 different types of receptor (Buck and Axel, 1991). In the olfactory bulb (OB) of the brain, axons of OSNs expressing different ORs sort out and project with precision to defined axon convergence sites (the glomeruli) topographically (Mombaerts et al., 1996; Ressler et al., 1994; Wang et al., 1998; Vassar et al., 1994). OSN projections between the olfactory epithelium (OE) and the OB are organized in at least two additional ways. First, axons of OSNs expressing the same OR converge to glomeruli located on the medial and the lateral side of the OB, respectively. This organization gives rise to two mirror-image sensory maps within each bulb (Nagao et al., 2000). Second, OE is divided into at least four OR expression zones, each with scattered OSNs that are specified to express one OR gene from a defined zonal set of OR genes (Ressler et al., 1993; Vassar et al., 1993). Evidence that axons of OSNs located in a particular OR zone terminate in a defined zone in the OB has come from the identification of the Rb8 neural cell adhesion molecule, RNCAM (NCAM2 – Mouse Genome Informatics) (Alenius and Bohm, 1997; Yoshihara et al., 1997). RNCAM is not expressed in OR zone 1 (Z1), while neurons located in OR zones 2, 3 and 4 [Z2-4, according to zone nomenclature of Ressler et al. (Ressler et al., 1993)] express RNCAM. The OB is thus divided into two main regions innervated by RNCAM-negative (Z1) and RNCAM-positive (Z2-4) axons. Owing to the capacity to mediate homophilic cell adhesion, it has been hypothesized that RNCAM regulates an initial level of selective guidance, by grouping Z2-4 axons together (Alenius and Bohm, 1997; Lin and Ngai, 1999; Yoshihara et al., 1997). Immunoreactivity corresponding to RNCAM disappears from axons after odor stimulation (Yoshihara et al., 1993). Thus, the function of RNCAM in Z2-4 appears to be regulated by neural activity. RNCAM is related to NCAM, *Drosophila* Fasciclin 2 (Fas2) and Aplysia CAM (apCAM) in terms of sequence similarity and domain structure. Alternative splicing generates isoforms with different attachments to the cell surface [i.e. by a glycosyl-phosphatidylinositol (Gpi) anchor or a transmembrane (Tm) domain]. Although subcellular localization, signaling and activity regulation are known to differ between Gpi and Tm

isoforms of NCAM-related proteins (Walsh and Doherty, 1997), little is known about their combined activities within a given cell type.

To study the importance of RNCAM isoforms in olfactory map formation, we have used the olfactory marker protein (OMP) gene promoter to generate transgenic mice with ectopic (in Z1) and elevated (in Z2-4) expression of either GpiRNCAM or TmRNCAM in OSNs. Our identification of NADPH diaphorase (NADPHd) activity as a novel marker for Z1 axons and the use a genetically modified mouse (P2-IRES-tau*lacZ*) (Mombaerts et al., 1996) have allowed us to conclude that OMP-RNCAM transgenic mice have an intact regional division of axon projections while showing errors in OR-specific axon segregation. The topographic distribution of glomeruli with axons having more than one OR identity in mice overexpressing either of the two RNCAM isoforms alone or in combination, suggest that OSNs use a dual, isoform-specific, regulatory function of RNCAM when precisely selecting target glomeruli.

MATERIALS AND METHODS

Generation of transgenic mice

To minimize risk of generating an artificial 5′ untranslated region that could interfere with translation, we cloned the second codon of RNCAM in frame with the initiation codon of OMP. An oligonucleotide that spanned from a *Bam*HI site at –75 to start codon of the OMP gene was ligated in-frame with a sequence containing GpiRNCAM-coding sequence and 78 bp of 3′ untranslated region (UTR). A SV40 polyadenylation site was introduced between the *Eco*RI site in the RNCAM sequence and the *Sma*I site in the cloning vector (pBSK, Stratagene, La Jolla, CA). This construct was used to generate a TmRNCAM transgene construct by replacing 354 bp of sequence unique to GpiRNCAM with a fragment that contained 538 bp 3′ coding region and 268 bp 3′ UTR unique to TmRNCAM. Finally, a *Bam*HI fragment (–6000 to –75) of mouse genomic OMP was ligated to *Bam*HI-*Bgl*II sites within the plasmids containing GpiRNCAM and TmRNCAM cDNA, respectively. After sequencing, transgenic constructs were gel purified and microinjected into pronuclei of C57/B6/CBA one-cell embryos. Two and three founder lines were generated that expressed the Tm and Gpi isoform of RNCAM, respectively. Transgenic founder mice were backcrossed to C57/B6 and the F1 generation from crosses between RNCAM transgenic mice and P2-IRES-tau-*lacZ* mice were used in phenotypic characterization. The littermate control mice analyzed were therefore not genetically identical to the parental P2-IRES-*taulacZ* (Mombaerts et al., 1996) mouse strain which might explain subtle differences in number of P2 glomeruli.

Generation of the anti-RNCAM antibody

A pBAD (Invitrogen, Carlsbad, CA) vector was used to generate a Myc/His-tagged TmRNCAM protein that corresponded to amino acid residues 442-685 in the extracellular domain. Bacterial expression (strain Top10, Invitrogen, Carlsbad, CA) was induced with 1% Arabinose (Sigma-Aldrich, Sweden) at 37°C for 1 hour. Bacteria was sonicated and tagged peptide was recovered on Ni-NTA agarose (Qiagen, Germany). Rabbits were immunized with 500 μg of purified protein followed by several boosting injections with 100 μg of protein (Agrisera, Sweden). Antiserum was purified using a column of Top 10 bacterial extract coupled to CNBr Sepharose (Amersham Pharmacia Biotech, Sweden) and subsequently affinity purified by binding and elution from a column of tagged RNCAM protein coupled by cyanogen bromide (BioRad, Sweden). Specificity of purified anti-RNCAM antibody was confirmed by western blot analyses using homogenates from olfactory bulb and brain.

Immunocytochemistry

Tissue from 2-week-old mice was fixed in 4% paraformaldehyde/PBS for 30-90 minutes at room temperature and decalcified in 0.5 M EDTA at 4°C for 3-10 days. Tissue was cryoprotected by 30% sucrose at 4°C for 24 hours, embedded in OCT compound (Sakura Finetek, Torrance, CA) and cryosectioned (16 μm). Retrieval of RNCAM antigen was achieved by microwaving at 650 W for 10 minutes in 10 mM citrate buffer (pH 6.0). Sections were incubated for 1 hour at room temperature in blocking solution (3% normal goat serum, 0.1 M phosphate buffer, 2 mM $MgCl_2$, 5 mM EGTA, 0.02% Nonidet P-40, and 0.001% sodium deoxycholate) followed by an overnight incubation at 4°C in blocking solution containing affinity-purified anti-RNCAM antibody (1:100). Sections were subsequently washed with PBS and a positive immunoreaction was visualized by using biotinylated goat anti-rabbit IgG (1:250) (Vector laboratories, Burlingame, CA) and Cy3-coupled strepavidin (1:2000) (Jackson Immuno Research laboratories, West Grove, PE) for 1.5 hours and 30 minutes, respectively. Sections were counter stained with Hoechst 33258 (Sigma-Aldrich, Sweden) and mounted with Dako fluorescent mounting media (Dako, Sweden). Microphotographs were taken using fluorescent optics on a Zeiss Axioskop microscope (Zeiss, Sweden)

In situ hybridization

Pretreatment of sections was carried out according to Breitschopf et al. (Breitschopf et al., 1992). Cryosections (10 μm) were hybridized to ^{35}S-labelled RNCAM cRNA probes; hybridization and washing conditions were as described previously (Sassoon et al., 1988). The probe that recognized both isoforms of RNCAM corresponded to a 1.4 kb fragment coding for the extracellular RNCAM domain. Isoform-specific probes corresponded to published sequences of GpiRNCAM (bp 2204-2900, Accession Number, AF016619) and TmRNCAM (bp 312-842, Accession Number, AF016620), respectively. Slides were dehydrated and processed for autoradiography using NTB-emulsion (Kodak, Sweden), and exposed for 5-14 days at 4°C. Histological staining of sections was performed with the nuclear dye Hoechst, and analysis was carried out using both fluorescent and dark-field optics on a Zeiss Axioskop microscope.

NADPH diaphorase and β-galactosidase histochemistry

NADPH diaphorase histochemistry was carried out essentially as previously described (Dellacorte et al., 1995). Cryosections (16-40 μm) of OE and OB were mounted on slides, washed twice with 100 mM Tris HCl (pH 8.0), incubated for 60 minutes at 37°C in 1 mM β-NADPH, 0.3% Triton X-100, 1.5 mM L-Arginine, 0.8 mM NBT 100 mM Tris-HCl (pH 8.0), rinsed in PBS and counterstained with Hoechst. β-Galactosidase histochemistry was carried out on serial coronal OB cryosections (40 μm). Slides were rinsed three times for 20 minutes in 0.1 M phosphate buffer, 2 mM $MgCl_2$, 5 mM EGTA, 0.02% Nonidet P-40, and 0.001% sodium deoxycholate. The staining reaction was carried out in the same buffer, supplemented with 1 mg/ml X-gal, 5 mM K_3 $Fe(CN)_6$, and 5 mM K_4 $Fe(CN)_6$, overnight (16 hours) at 37°C. Sections were subsequently rinsed three times in PBS, counterstained with Hoechst and mounted with Dako farmount mounting media (Dako, Sweden). Student's *t*-test (two tailed) was used to determine statistical significance of all morphological data sets.

RESULTS

Generation of transgenic mice with increased RNCAM expression in OSNs

Alternative splicing leads to generation of two RNCAM isoforms with different methods of cell membrane attachment: a Tm domain and a Gpi-anchor. In order to study the function

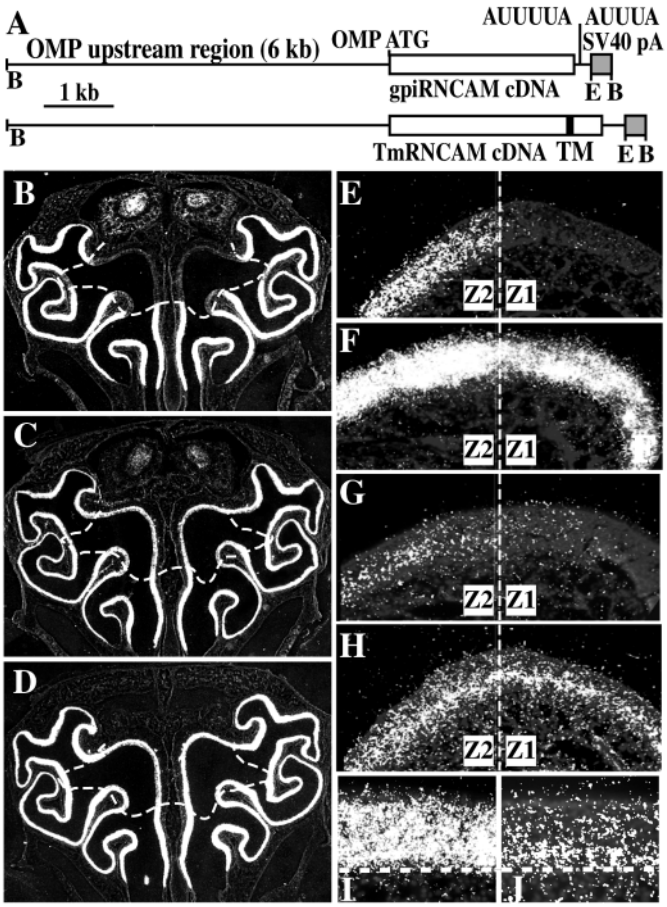

Fig. 1. Expression of transgenic and endogenous RNCAM isoforms in OSNs. (A) Schematic representation of OMP-GpiRNCAM and OMP-TmRNCAM transgene constructs. A 6.0 kb mouse genomic OMP sequence that spanned from an endogenous *Bam*HI (B) site to the OMP initiation codon was cloned in frame with RNCAM cDNA coding sequence (white boxes). The cDNA corresponded to sequences between initiation codons and endogenous *Eco*RI (E) sites in the 3′ UTRs of GpiRNCAM and TmRNCAM transcripts, respectively. Indicated are SV40 polyadenylation sites (SV40 pA, gray boxes), the transmembrane domain (TM) and two AU-rich boxes in the 3′ UTR of the GpiRNCAM transcript. (B-H) In situ hybridization analyses of RNCAM expression in OE. Hybridization signals appear white after darkfield illumination. (B-D) Coronal sections of 2-week-old mice hybridized with a probe corresponding to the extracellular domain of RNCAM, common to both isoforms. Broken line indicates the Z1-Z2-border. RNCAM expression in OE of (B) control mouse, (C) GpiRNCAM transgenic mouse and (D) TmRNCAM transgenic mouse are shown. (E-H) Higher magnification of in situ hybridization analyses of RNCAM isoforms in transgenic mice. Sections were hybridized with a TmRNCAM-specific probe (E-F) or a GpiRNCAM-specific probe, (G-H). Signals corresponds to endogenous TmRNCAM expression in GpiRNCAM transgenic mice (E), endogenous and transgenic TmRNCAM expression in TmRNCAM transgenic mice (F), endogenous GpiRNCAM expression in TmRNCAM transgenic mice (G) and endogenous and transgenic GpiRNCAM expression in GpiRNCAM transgenic mice (H). The Z1-Z2 border (broken line) in transgenic mice was determined by hybridizing serial sections with probes corresponding to the isoform not overexpressed from the transgenic construct. E and H are serial OE sections of GpiRNCAM transgenic mice, while F and G are serial OE sections of TmRNCAM transgenic mice. In situ hybridization analyses shown in E-H were generated from sections that were processed, hybridized and exposed identically and in parallel. Results from analyses of two transgenic mouse lines for each RNCAM isoform were consistent. (I,J) Laminar distribution in OE of endogenous RNCAM mRNA isoforms. In situ hybridization analyses of serial OE sections of control mice. (I) In situ hybridization signal generated with a ^{35}S-labeled cRNA probe that recognized TmRNCAM transcripts throughout all cell layers of OSNs. (J) In situ hybridization with a ^{35}S-labeled cRNA probe that recognized GpiRNCAM transcripts preferentially located in the cell layer of OE containing immature OSNs close to the basal lamina (broken line).

of RNCAM isoforms in olfactory map formation, we generated transgenic founder lines expressing either of the two isoforms. To ensure specific expression in OSNs we used a transgene construct containing SV40 poly-adenylation sites and a 6 kb mouse genomic fragment corresponding to the region upstream of OMP coding sequence (Fig. 1A). The rat and mouse OMP promoters have been shown to drive expression efficiently of transgenes in OSNs throughout the OE (Danciger et al., 1998; Servenius et al., 1994). Two transgenic founder lines for each RNCAM isoform were analyzed in detail. In situ hybridization analyses showed that in all four lines, RNCAM expression was evident in this zone (Fig. 1B,D). As endogenous RNCAM is not expressed in the most dorsomedial OR zone (Z1), ectopic expression of transgenic RNCAM was evident in this zone (Fig. 1B-D). Demonstration of increased total (i.e. endogenous plus transgenic) levels of RNCAM mRNA splice variants in OR zones 2-4 required comparative analyses on serial tissue sections using isoform-specific probes. Ectopic levels of RNCAM in Z1 were higher than endogenous RNCAM mRNA levels detected in Z2-4, e.g. compare endogenous TmRNCAM levels (Fig. 1E, Z2) with transgenic TmRNCAM levels (Fig. 1F, Z1) and endogenous GpiRNCAM levels (Fig. 1G, Z2) with transgenic GpiRNCAM levels (Fig. 2H, Z1). From these experiments, we concluded that transgenic animals expressed RNCAM mRNA ectopically in Z1 OSNs, whereas Z2-4 OSNs demonstrated increased levels of RNCAM mRNA.

Immature OSNs are located close to the basal cell layer of OE. A probe specific for TmRNCAM hybridized to OSNs in OE layers containing both immature and mature OSNs, whereas a GpiRNCAM-specific probe hybridized predominantly to immature OSNs (Fig. 1I,J). This result indicated that RNCAM isoforms showed a different laminar distribution in OE because of post-transcriptional regulation of mRNA steady-state levels. Surprisingly, the same distribution of RNCAM isoforms was evident in transgenic mice (Fig. 1F,H). Thus, exogenous and endogenous RNCAM transcripts showed the same relative distribution in OE, regardless of the fact that the gene regulatory sequences determining transcription were different, i.e. OMP or RNCAM promoters, respectively. As cDNA of spliced transcripts was used to construct the transgenes, the result indicated that the observed difference in distribution of RNCAM mRNA isoforms was regulated by differential mRNA stability and not differential splicing. Because both transgenes contained an identical 5′ UTR, the results further suggested that the determinant regulating the differential mRNA stability was located within the 3′ UTRs that differed. The turnover of an mRNA can be regulated by cis-acting elements located in the 3′ UTR such as

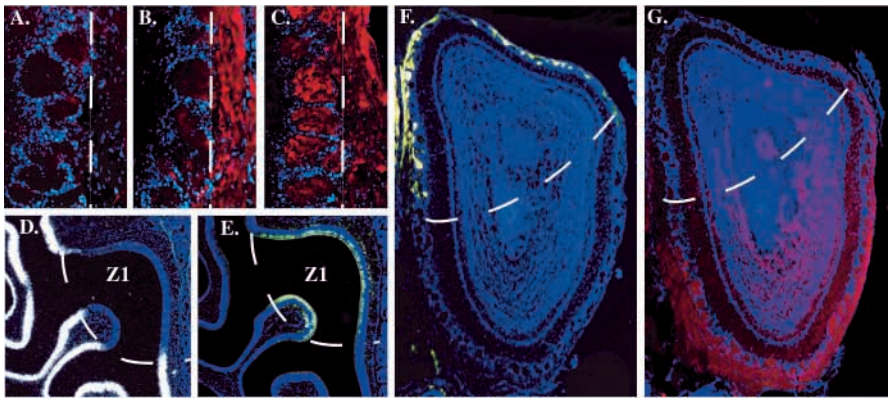

Fig. 2. Distinct distribution of RNCAM isoforms on axons of OSNs and Z1-specific NADPHd-activity. Images were processed to show RNCAM immunoreactivity in red, RNCAM in situ hybridization signal in white, NADPHd-activity in yellow and nuclear counterstain in blue. (A-C) Anti-RNCAM immunohistochemistry analyses of nerve and glomeruli layers in a region of the OB innervated by Z1 axons lacking endogenous RNCAM expression in (A) control mice lacking RNCAM immunoreactivity, (B) GpiRNCAM transgenic mice with RNCAM immunoreactivity predominantly localized to the in nerve layer, and (C) TmRNCAM transgenic mice with RNCAM immunoreactivity localized to both nerve and glomerular layers. The broken line indicates the border between the two layers. (D) In situ hybridization analyses showing RNCAM expression in Z2-4; (E) NADPHd histochemistry analyzes showing a signal selectively confined to Z1 OSNs (Z1). Note the complementary signals on either side of the Z1/Z2 border (broken line). (F) NADPHd histochemistry analysis showing signal in the nerve and the glomerular layers of the OB. (G) Anti-RNCAM immunohistochemistry analysis showing RNCAM immunoreactivity in the nerve and the glomerular layers of the OB. Note the complementary signals on either side of the broken line. Experiments were carried out using serial coronal sections of OE (D,E) and OB (F,G).

the AU-rich elements (AREs) that are binding sites for proteins regulating mRNA turnover (Ross, 1995). Interestingly, two AREs (AUUUA and AUUUUA) were present within the 3′ UTR unique to the GpiRNCAM construct (Fig. 1A). It has been shown that the expression of *Gap43* (*Basp2* – Mouse Genome Informatics) mRNA is regulated post-transcriptionally via AREs and that the protein is synthesized in high amount during neurite outgrowth (Beckel-Mitchener et al., 2002). In this respect, it is interesting to note that we found GpiRNCAM mRNA to be expressed in the same cell layer of OE as *Gap43* mRNA (Verhaagen et al., 1989). These results suggested that the GpiRNCAM isoform might function in axons of immature OSNs, while TmRNCAM in addition might have a function in more differentiated OSNs.

In tissue sections of the OB, the GpiRNCAM-specific probe generated no hybridization signal above background, while the TmRNCAM-specific probe generated a hybridization pattern indistinguishable from that reported for a probe recognizing both isoforms (Alenius and Bohm, 1997; Yoshihara et al., 1997). Thus, TmRNCAM appears to be evenly distributed along the dorsoventral and mediolateral extensions of granular, mitral and periglomerular cell layers.

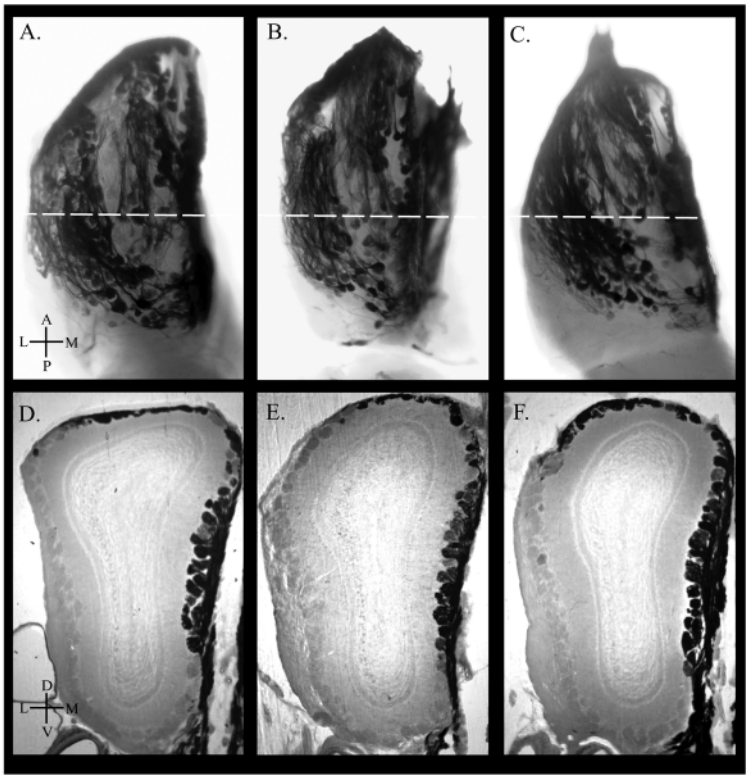

Differential distribution of Gpi and Tm RNCAM protein

We generated a polyclonal antiserum against the common extracellular domain. To analyze for cellular distribution of RNCAM isoforms, we took advantage of the fact that Z1 OSNs lack endogenous RNCAM. As expected, control mice showed no RNCAM immunoreactivity in Z1 glomeruli (Fig. 2A). For GpiRNCAM transgenic mice, intense immunoreactivity was observed in the nerve layer, whereas glomeruli showed less staining (Fig. 2B). Thus, when GpiRNCAM was expressed at levels higher than normal, this isoform

Fig. 3. Unaltered distribution of NADHPd-positive glomeruli in RNCAM transgenic mice. (A-F) Histochemistry analyzes of NADPHd activity (black) in the OB. (A-C) Dorsal views of whole-mount OB preparations; control mouse (A), GpiRNCAM transgenic mouse (B) and TmRNCAM mice (C). (D-F) Coronal sections of the OB at a rostrocaudal position indicated by a broken line in A-C from control mouse (D), GpiRNCAM transgenic mouse (E) and TmRNCAM transgenic mice (F). Although the intensity and exact position of NADPHd-positive glomeruli varied between individual mice in an RNCAM-independent manner, both control and RNCAM-transgenic mice showed an identical general topography of NADPHd-positive and NADPHd-negative OB regions.

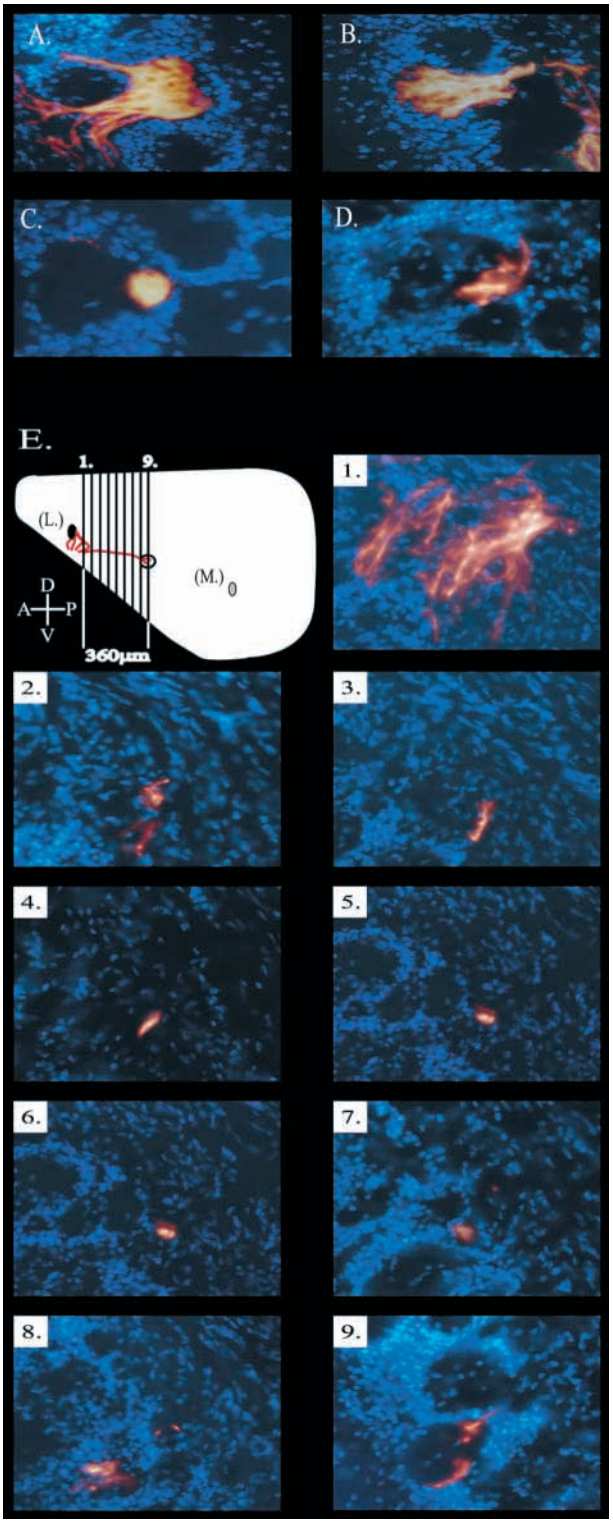

Fig. 4. Glomerular morphology and trajectory of misrouted P2 axons in GpiRNCAM transgenic mice. (A-D) High power images of P2 innervated glomeruli. Major P2 glomeruli showed a similar morphology in control mouse (A) and GpiRNCAM transgenic mouse (B). An increased number of a distinct type of P2 glomeruli, in which P2 axons contributed only fractionally to the total number of innervated axons, were detected in transgenic mice. These semi-innervated P2 glomeruli showed a similar morphology in mice heterozygous (C) and homozygous (D) for the targeted P2 allele. (E) Location (vertical lines) of serial coronal sections shown in E1-9. The semi-innervated P2 glomeruli analyzed was located 360 μm caudal to the major lateral P2 glomeruli. The drawing depicts a side view, with the major lateral P2 glomerulus (L), axon trajectory of P2 axons (red line) and semi-innervated P2 glomeruli (circle) located on the lateral side, whereas the major medial P2 glomerulus (M) is located on the opposite (medial) side of the olfactory bulb. (E1-9) High power images of serial coronal olfactory bulb sections from a GpiRNCAM transgenic mouse. Misguided P2 axons segregated from a lateral division of P2 axons close to the major lateral P2 glomerulus (E1), bypassed their correct target and coursed in a caudal and ventral direction (E2-7) to a glomerulus primarily innervated by axons of another OR specificity (E8-9). Photographs were processed to show β-galactosidase staining in red, while UV visualized the nuclear counterstain in blue.

preferentially localized to axons in the nerve layer. This result indicated that the immunoreactivity in Z2-4 glomeruli of control mice corresponded to TmRNCAM and not GpiRNCAM (Fig. 2G). The finding that transgenic TmRNCAM protein showed equally strong immunoreactivity in nerve and glomerular cell layers supported this notion (Fig. 2C). The differential distribution of RNCAM isoforms may relate to the fact that Gpi-anchored proteins, in contrast to many transmembrane proteins, are clustered in sphingolipid-sterol rich microdomains or rafts that influence subcellular localization (Simons and Ikonen, 1997). An alternative interpretation is that the levels of expression per se determine the axonal distribution of RNCAM isoforms. The finding that endogenous expression levels of TmRNCAM was higher than that of GpiRNCAM in control mice support such a notion (Fig. 1E,G). However, regardless of the mechanism causing the differential distribution observed, the results suggested that both isoforms were present on axons in the nerve layer, whereas TmRNCAM was the predominant isoform on axon terminals within glomeruli.

Unaltered Z1 topography in Gpi and Tm RNCAM transgenic mice

Our analyses addressing whether gain of RNCAM function alters the broad zonal organization of projections were hampered by the fact that no marker, except RNCAM, had been identified that distinguish this division. Previous studies have reported that NADPH diaphorase (NADPHd) activity is restricted to the dorsomedial OE and OB (Davis, 1991; Dellacorte et al., 1995). In situ hybridization analysis of RNCAM and NADPHd histochemistry on serial sections of OE revealed that NADPHd activity was complementary to RNCAM expression and thus restricted to Z1 (Fig. 2D,E). Importantly, no RNCAM/NADPHd double-positive glomerulus was found (Fig. 2F,G). Besides the intriguing topographical restriction of NADPHd-activity, this represented a useful marker for the majority of Z1 axons and their terminals in the OB. Fig. 3 shows comparisons of NADPHd activity in whole-mount preparations, as well as serial OB sections of transgenic mice and littermate controls. These analyses revealed that control mice (Fig. 3C,F) and transgenic mice (Fig. 3A,B,D,E) had equal surface areas and spreading of the NADPHd-positive region along dorsoventral, mediolateral and rostrocaudal axes of the OB. Moreover, no NADPHd-positive

glomeruli or stray axons were present in the region of the bulb that normally is innervated by RNCAM-positive axons. This indicated that topographic expression of RNCAM does not determine the division of the glomerular field into two major regions that receive input from OSNs located in Z1 and Z2-4.

A fraction of P2 axons targets incorrect glomeruli

As RNCAM-mediated adhesion theoretically can interfere with a number of different axon guidance decisions, we analyzed the projections from one defined OSN subpopulation (P2) in detail. The P2 OR gene is expressed by RNCAM-positive OSNs located in Z2. Axons of the P2-positive OSN subpopulation can be visualized with the aid of the P2-IRES-tau-*lacZ* mouse line, which was generated by gene replacement in embryonic stem cells described by Mombaerts et al. (Mombaerts et al., 1996). This mouse line has a P2 allele that is modified to express a bicistronic transcript generating normal P2 OR protein, as well as an easily visualized reporter protein (the microtubule-associated protein tau fused to β-galactosidase). Histochemical staining for β-galactosidase activity allows for direct visualization of P2 axons. We analyzed mice carrying one copy of the P2-IRES-tau-*lacZ* allele together with one RNCAM transgene allele, either OMP-TmRNCAM or OMP-GpiRNCAM. P2 axons were visualized in coronal sections of nasal tissue and OB of 2-week-old mice. Transgenic and control mice had equal total numbers of morphologically similar P2 glomeruli (Fig. 4A,B; Fig. 5A). Interestingly, examination of transgenic mice revealed increased numbers of a type of glomeruli that was only partially innervated by P2 axons (Fig. 4C,D). It has been reported that intermingling of axons corresponding to two closely related ORs occurs during early postnatal development, while misrouted axons are rarely detected in adult animals (Conzelmann et al., 2001; Mombaerts et al., 1996; Potter et al., 2001; Royal and Key, 1999). Royal et al. have however, reported a sporadic occurrence of semi-innervated P2 glomeruli in which P2 axons appear to terminate in a discrete subregion of the glomerulus, either with a diffuse or dense distribution (Royal and Key, 1999). The increased number of such semi-innervated P2 glomeruli in transgenic mice indicated that gain of RNCAM function augmented the frequency at which such axonal targeting errors occur. We estimated the number of this type of glomeruli to be on average 0.6 per OB in 2-week-old control mice and 1.5-2 per OB in RNCAM transgenic littermates (Fig. 5B).

Axons of P2 OSNs typically innervate one glomerulus (or a few juxtaposed glomeruli) on the medial and lateral sides of each bulb. Thus, each wild-type P2-IRES-tau-*lacZ* mouse has at least four fully innervated glomeruli (Mombaerts et al., 1996). In our experimental system, we detected on average five fully innervated glomeruli per control mouse. It has been speculated that the variation in the exact number of glomeruli might be a reflection of genetic background differences and/or variations in the odorous environment of animal facilities (Potter et al., 2001). It is conceivable that the occurrence of semi-innervated P2 glomeruli in control mice will vary between laboratories for the same reasons. To control for genetic background and odor environment, we performed all quantitative analyses on transgenic and control littermates. As an additional control, we analyzed an OMP promoter-driven transgenic mouse line that overexpressed a cell-surface protein (neuropilin 2) unrelated to RNCAM (data not shown). Transgenic OMP-neuropilin 2 mice and littermate controls

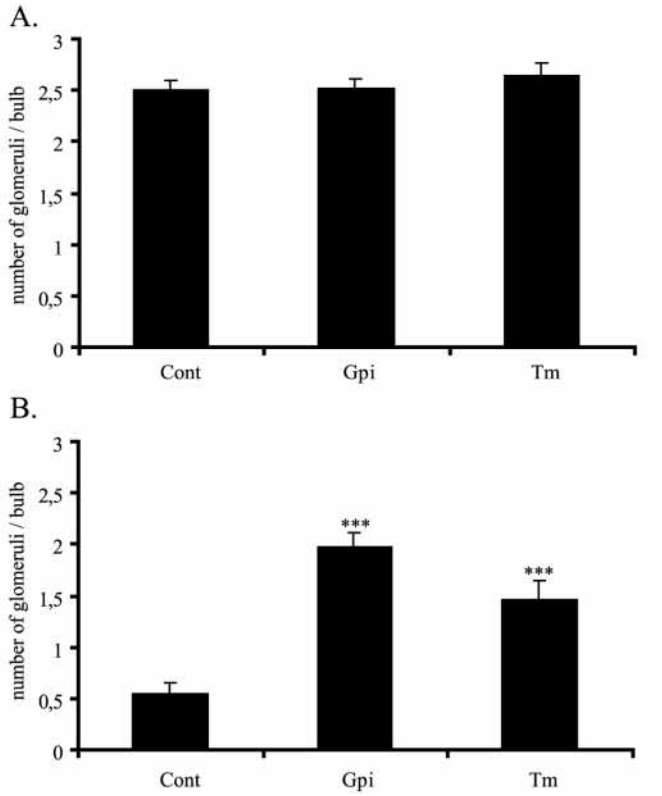

Fig. 5. Increased number of semi-innervated P2 glomeruli in transgenic mice. Quantification of glomeruli in control and transgenic mice. P2 axons were visualized by β-galactosidase staining and innervated glomeruli were counted manually. (A) Graph represents total number of major P2 glomeruli/olfactory bulb in control (cont) (*n*=36), GpiRNCAM (Gpi) (*n*=42) and TmRNCAM (Tm) (*n*=26) transgenic animals. Control and transgenic mice had the same number of major glomeruli. (B) Graph represents total number of semi-innervated P2 glomeruli/olfactory bulb in control mice (cont) (*n*=36), GpiRNCAM (Gpi) (*n*=42) and TmRNCAM (Tm) (*n*=26) transgenic animals. Both GpiRNCAM and TmRNCAM transgenic mice showed a significant increased number of semi-innervated P2 glomeruli. Results are mean±s.e.m. (***P<0,0001, Student's *t*-test). The data were obtained from progeny of two transgenic founder lines transgenic for each RNCAM isoform.

were found to have the same number of semi-innervated P2 glomeruli 0.7±0.2 per OB (SEM, *n*=10) and 0.6±0.2 per OB (SEM, *n*=8), respectively. These results showed that the increased number of targeting errors was an effect specific to RNCAM overexpression.

OR genes are subject to the phenomenon of monoallelic expression (Chess et al., 1994). Appearance of semi-innervated P2 glomeruli in mice homozygous or heterozygous for the targeted P2 allele was similar (Fig. 4D). This excluded the possibility that the unstained fraction of axons in the semi-innervated P2 glomeruli exclusively corresponded to OSNs that express P2 from the untargeted P2 allele because of allelic inactivation. Moreover, the OE in RNCAM transgenic mice had a normal structure and normal expression of NADPHd activity, endogenous RNCAM (Fig. 1E,F,G,H), neuropilin 2 and OR genes specific for Z1 (K21), Z2 (P2, K20), Z3 (L45) and Z4 (A16) (data not shown). These results taken together with the predominant localization of RNCAM protein on axons

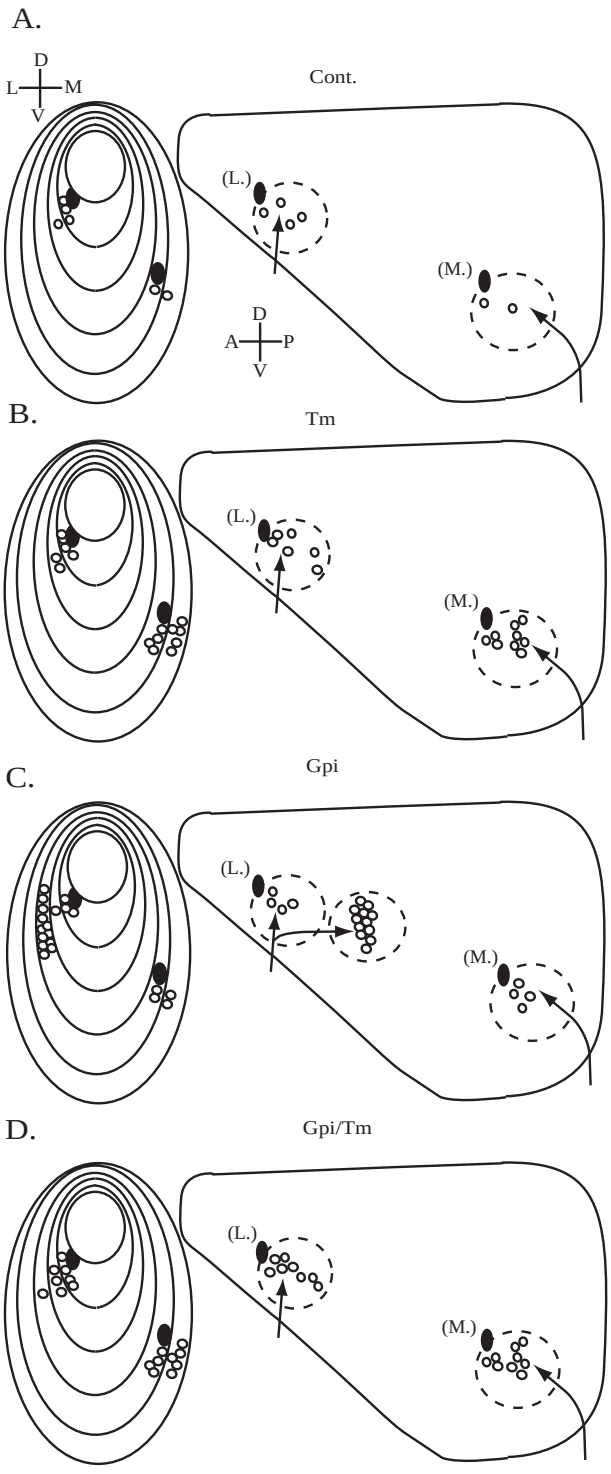

Fig. 6. Two distinct RNCAM isoform-dependent activities influence segregation of P2 axons. Frontal (left) and side view (right) of olfactory bulb. The location of P2 semi-innervated glomeruli (white circles) relative to major lateral (L) and medial (M) P2 glomeruli (black circles) are shown in ten mice of each genotype. (A) Control mice (cont), (B) TmRNCAM transgenic mice (Tm), (C) GpiRNCAM transgenic mice (Gpi) and (D) double GpiRNCAM/TmRNCAM transgenic mice (Gpi/Tm). Three different domains (broken circles) of the OB, with an approximately diameter of 200 μm, contained semi-innervated P2 glomeruli. The trajectories of P2 axons innervating incorrect glomeruli within the domains are indicated with arrows. Note that overexpression of TmRNCAM results in targeting errors in close proximity to both the medial and the lateral P2 glomeruli within a domain in which spontaneous targeting errors can be found at a low frequency in control mice. Overexpression of GpiRNCAM results in targeting errors located caudally, distant from the main lateral P2 glomeruli. The phenotype of mice overexpressing both RNCAM isoforms is similar to that of TmRNCAM transgenic mice. These results indicate that two independent RNCAM isoform-specific mechanisms influence OR-specific axon segregation. The data were obtained from progeny of two transgenic founder lines transgenic for each RNCAM isoform.

indicate that the increased number of incorrectly targeted P2 glomeruli was a consequence of aberrant axon navigation within the OB, rather than disorganization of OSNs within the OE itself.

Isoform-specific effect on topography of axon navigational errors

Interestingly, we detected a three- to fourfold increase of incorrectly targeted glomeruli in both TmRNCAM and GpiRNCAM transgenic mice (Fig. 5B). A close examination of the distribution of semi-innervated P2 glomeruli revealed that they were confined to different domains of the OB, depending on which isoform was overexpressed. In control mice, sporadic semi-innervated P2 glomeruli were located within domains of the glomerular field that could be represented by circles with a diameter of 200 μm being centered 100 μm caudoventral to the major P2 glomeruli (i.e. in the vicinity of the major P2 glomeruli) (Fig. 6A). The increase of semi-innervated P2 glomeruli detected in TmRNCAM transgenic mice occurred within the same domains (Fig. 6B; Fig. 7). Although semi-innervated P2 glomeruli in control mice were slightly biased to the lateral side, the reverse was true in TmRNCAM transgenic mice (Fig. 6A,B; Fig. 7). Notably, a different pattern was evident in GpiRNCAM transgenic mice. In these mice, semi-innervated P2 glomeruli were predominantly located within a domain with a diameter of approximately 200 μm, centered 340 μm caudoventral to the major lateral P2 glomeruli (Fig. 6C; Fig. 7). The result indicated that elevated levels of TmRNCAM enhance a type of axon targeting error that occurs normally close to the major P2 glomeruli, while elevated levels of GpiRNCAM result in a different type of aberrant axon navigation and targeting (se below). Moreover, TmRNCAM predominantly affected axons projecting to the medial map, while GpiRNCAM selectively affected P2 axons to target incorrect glomeruli within a domain distant to the main lateral P2 glomeruli.

The location of an OR-specific glomerulus is almost constant between individuals but some variations do occur (Schaefer et al., 2001; Strotmann et al., 2000). This local permutation in the glomerular array precluded a precise determination of whether P2 axons co-converged with axons of OSNs expressing the very same OR gene in different mice. Importantly however, semi-innervated P2 glomeruli in GpiRNCAM transgenics showed a similar location in different mice, i.e. 330±16 μm (n=22) relative to the major lateral P2 glomeruli. Using the same way of measuring revealed a distance of 705±18 μm (n=22) between major medial and

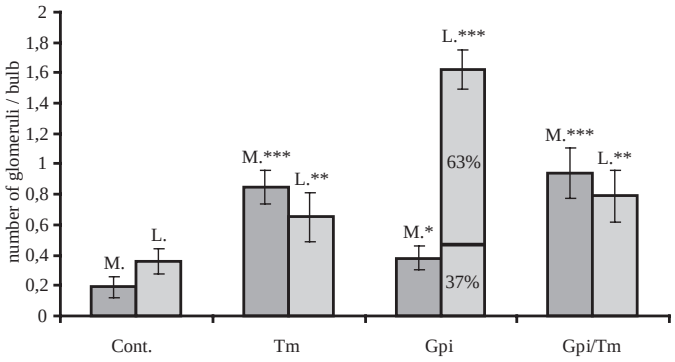

Fig. 7. RNCAM isoform-dependent variations in the number of laterally and medially located semi-innervated P2 glomeruli. Number of semi-innervated P2 glomeruli was quantified on serial sections of olfactory bulb stained for β-galactosidase activity. Graphs represent total number of semi-innervated P2 glomeruli located in the medial (M) and lateral (L) hemisphere of the olfactory bulb in control mice (cont) (n=36), TmRNCAM transgenic mice (Tm) (n=26), GpiRNCAM transgenic mice (Gpi) (n=42) and TmRNCAM/GpiRNCAM (Gpi/Tm) double transgenic mice (n=16). Results are mean±s.e.m. ***P<0.0001, **P<0.005, *P<0.05; Student's t-test. The fractions of semi-innervated P2 glomeruli located proximal (37%) and caudal (63%) to the main lateral P2 glomerulus in GpiRNCAM transgenic mice were calculated from analyses (shown in Fig. 6) that were carried out to determine both rostrocaudal and mediolateral distances. The data were obtained from progeny of two transgenic founder lines transgenic for each RNCAM isoform.

lateral P2 glomeruli. These results then indicated that the positions of invariant P2 glomeruli and semi-innervated P2 glomeruli showed a similar degree of local permutation. The GpiRNCAM-specific phenotype thus appeared to be a consequence of co-convergence of P2 axons with axons corresponding to a limited set of OR identities.

Axons forming P2 semi-innervated glomeruli in GpiRNCAM mice 'bypass' major lateral glomeruli

The trajectories of axons forming semi-innervated P2 glomeruli in GpiRNCAM mice was followed from the glomeruli towards OE by analyzing serial sections of the OB (Fig. 4E). Some P2 axons segregated from the lateral division of P2 axons close to the major lateral P2 glomeruli. These misguided P2 axons thus bypass their target, turn posteriorly, course in an ventral direction and innervate a glomerulus with an OR specificity that is different from P2 (Fig. 6C). Examination of P2 axons forming semi-innervated glomeruli in TmRNCAM transgenic and control mice revealed a different type of trajectory. Instead of bypassing the correct target glomeruli, P2 axons terminated within incorrect glomeruli on the way towards the correct target glomeruli (Fig. 6B; Fig. 8). An estimation of the location of semi-innervated P2 glomeruli by comparative NADPHd histochemistry on serial sections revealed that incorrectly targeted glomeruli were not in a region of the OB that corresponded to Z1 (Fig. 8). This result indicated that axons of a defined Z2 OSN subpopulation do not co-converge with axons of Z1 OSNs that ectopically express RNCAM. Thus, the result supported the conclusion that the Z1/Z2-4 division of the glomerular field is formed independently of spatial RNCAM expression.

Suppression of GpiRNCAM-specific targeting errors in Gpi/Tm double transgenic mice

An increased number of semi-innervated P2 glomeruli were detected in transgenic mice overexpressing either of the two RNCAM splice variants. This suggested that the isoforms fulfill similar functions. The results also suggested that TmRNCAM and GpiRNCAM have distinct functions as convergence errors were located to different domains of the OB, depending on isoform overexpressed. Interestingly, mating TmRNCAM and GpiRNCAM mice generated offspring with a phenotype similar to that of TmRNCAM transgenic mice. Thus, TmRNCAM/GpiRNCAM double transgenic mice showed an increased number of semi-innervated P2 glomeruli within a domain in the vicinity of major P2 glomeruli (Fig. 6D). Moreover, the increase was biased toward the medial P2 glomerulus, similar to the situation in transgenic mice overexpressing TmRNCAM only (Fig. 7). This result indicated that TmRNCAM inhibits formation of GpiRNCAM-specific targeting errors distal to the lateral P2 glomerulus. TmRNCAM, on the other hand, exhibits a GpiRNCAM-independent function that results in targeting errors proximal to major P2 glomeruli.

DISCUSSION

RNCAM is a homophilic cell adhesion molecule related to NCAM and invertebrate orthologs such as apCAM and Fas2. We show that RNCAM-negative axons and their terminals within glomeruli in the OB can be visualized by NADPHd histochemistry. This novel marker for Z1 axons has allowed us to address the function of zonally restricted expression of RNCAM in OE. Transgenic mice with ectopic RNCAM expression in Z1 and control mice show an indistinguishable topography of NADPHd-positive and NADPHd-negative OB regions. This finding indicates that Z1 axons project to the dorsomedial OB and avoid the ventrolateral part, irrespective of whether they express RNCAM or not. Conversely, we show that axons of a defined RNCAM-positive OSN subpopulation (P2) are not attracted to the NADPHd-positive (Z1) region of the OB in RNCAM transgenic mice. This indicates that RNCAM does not determine formation of a broad regional division of projections from OE to OB. A candidate molecule with such functions is the semaphorin receptor neuropilin 2, which was recently shown to mediate zonal segregation, but not axonal convergence, of olfactory sensory neurons located in the vomeronasal organ (Cloutier et al., 2002). Supporting the notion that other genes may regulate the formation of zone-specific projections in the main olfactory system is the finding that neuropilin 2 mRNA is expressed in a step gradient, with highest relative levels in Z4 and lowest in Z1 (Norlin et al., 2001).

If RNCAM does not determine formation of a broad regional division of projections, it is possible that the topographic distribution of RNCAM expression has evolved to play a role in axon convergence and/or structural plasticity for neurons in Z2-4. In fact, previous studies of OSN-expressing tagged ORs corresponding to a RNCAM-negative Z1 OR (M72) and a

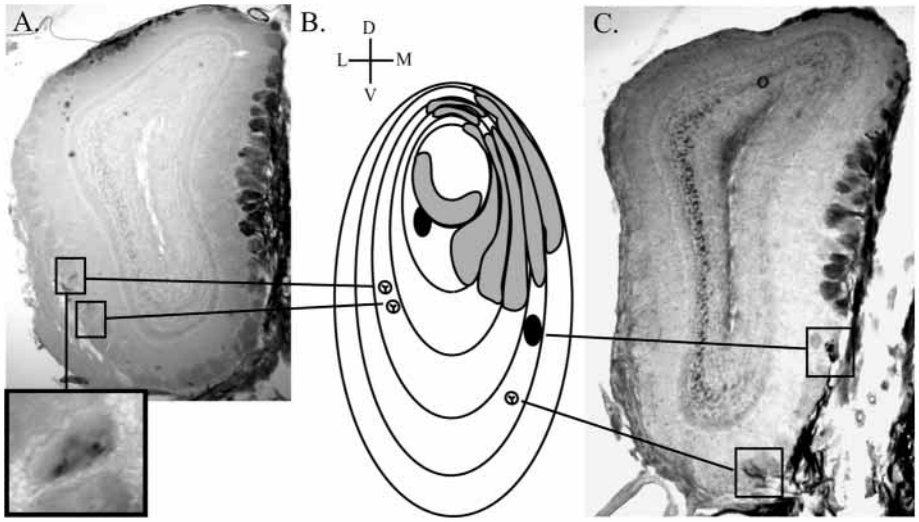

Fig. 8. Incorrectly targeted glomeruli are located in the NADPHd-negative region of OB. Shown are double NADPHd and β-galactosidase histochemistry analyses of coronal OB sections of a double GpiRNCAM/P2-IRES-tau-*lacZ* transgenic mouse. (A) Image of a rostral section with semi-innervated P2 glomeruli on the lateral side of the OB. One lateral semi-innervated P2 glomerulus (boxed) is shown at high magnification. (B) Schematic representation of NADPHd (gray) and β-galactosidase histochemistry (black) of P2 glomeruli on serial coronal sections throughout the rostrocaudal extension of the OB. Indicated are semi-innervated P2 glomeruli (white circles), major lateral and lateral P2 glomeruli (black circles). (C) Image of a rostral section with a semi-innervated P2 glomerulus located on the medial side of the OB. Semi-innervated P2 glomerulus and the major medial P2 glomerulus are boxed.

RNCAM-positive Z2 OR (P2) have provided evidence for heterogeneity in glomerular formation during development and sensitivity to targeted deletion of an olfactory cyclic nucleotide-gated channel subunit (Potter et al., 2001; Zheng et al., 2000). To determine if RNCAM function influences axon convergence, we have used the P2-IRES-tau-*lacZ* allele to probe for navigational errors of P2 axons. One finding is that increased expression of RNCAM in OSNs results in an increased number of glomeruli that are innervated by axons that represent more than one OR identity. This indicates that normal level of RNCAM is important for the formation of highly refined axon projections of OSNs, to which RNCAM expression is normally confined.

Alternative splicing generates two RNCAM isoforms that share an identical extracellular domain that mediates homophilic cell adhesion (Yoshihara et al., 1997). Different functions of RNCAM isoforms can be envisioned in light of the fact that TmRNCAM has a cytoplasmic domain that potentially could mediate signaling and/or coupling to the cytoskeleton (Walsh and Doherty, 1997). Like other Gpi-anchored proteins, GpiRNCAM may also affect intracellular signaling and not only represent adhesiveness as such (Davy et al., 1999). Interestingly, we find that overexpressing TmRNCAM increases the number of targeting errors of P2 axons within domains in the immediate vicinity of their original glomerular targets, while overexpression of GpiRNCAM results in semi-innervated P2 glomeruli located distant from the lateral P2 glomerulus. Moreover, TmRNCAM suppresses the GpiRNCAM-specific phenotype, while the reverse is not true for the TmRNCAM-specific phenotype. We interpret these results to suggest that topographic targeting of OR-defined axon subclasses is influenced by two distinct RNCAM-dependent mechanisms.

We find both isoforms of RNCAM expressed on axons in the nerve layer and the distribution of alternatively spliced transcripts in OE suggests that layers containing a high proportion of maturing OSNs express both isoforms. It is thus plausible that genetic interaction of GpiRNCAM and TmRNCAM is a consequence of their co-localization on axons in the nerve layer during axonal outgrowth and navigation. Misrouted P2 axons in GpiRNCAM transgenic mice bypass the correct glomerular target and turn caudally before defasciculating at an incorrect choice point, i.e. at a glomerulus with an OR identity different from P2. The resolution of the experimental system allows us to determine that incorrectly targeted glomeruli show a similar location in different individuals. This phenotype indicates that elevated levels of GpiRNCAM reduce the specificity of OR-specific target selection. Genetic analyses in *Drosophila* have shown that alteration in the degree of Fas2-mediated axon-axon attraction directly influences the ability of motor axons to respond to target-derived attractants and repellents (Fambrough and Goodman, 1996; Winberg et al., 1998). For example, the combined function of Fas2 and semaphorins is involved in controlling selective defasciculation important for target selection during the generation of neuromuscular connectivity (Winberg et al., 1998; Yu et al., 2000). The possibility that the mechanism of target selection in *Drosophila* is phylogenetically conserved, in order to be applicable for OR-specific axon segregation in mammals, is appealing given that neuropilin 2 expression correlates with OR zones (Cloutier et al., 2002; Norlin et al., 2001). A GpiRNCAM-mediated change in the balance between RNCAM and neuropilin 2-mediated axon-axon attraction and repulsion, respectively, may thus increase the probability of defasciculation of P2 axons in an region of the OB that corresponds to an incorrect OR zone.

Errant axons in TmRNCAM transgenic mice, unlike those in GpiRNCAM transgenic mice, terminate within incorrect glomeruli on the way towards the correct target glomeruli. Moreover, targeting errors were located close to medial and lateral P2 glomeruli within domains in which sporadic semi-innervated glomeruli are found also in control mice. Previous studies have shown that OSNs expressing related ORs belonging to the same zonal set tend to form glomeruli in close proximity to each other (Conzelmann et al., 2001; Malnic et al., 1999; Tsuboi et al., 1999). Analyses of tagged OR genes indicate that axons of highly related OR identities segregate from each other during a short postnatal phase and that only a

few misprojections can be detected in glomeruli close to the correct target glomerulus at 1 week of age (Conzelmann et al., 2001). It is thus conceivable that regulated levels of TmRNCAM influences precision of targeting within a domain of glomeruli with highly related OR identities or, alternatively, glomeruli that belong to the same zonal set of OR identities.

The finding that increased levels of TmRNCAM enhance one type, and suppress another type, of OR-specific targeting error is intriguing in light of the fact that presence of TmRNCAM on the axonal surface appears to be regulated. Yoshihara et. al. have reported that odor stimulation causes disappearance of immunoreactivity corresponding to an epitope (R4B12) of the rabbit ortholog of RNCAM (Yoshihara et al., 1993). Diminished RNCAM immunoreactivity is limited to axon terminals within glomeruli. The fact that we find TmRNCAM to be the predominant isoform in glomeruli opens up the possibility that TmRNCAM and not GpiRNCAM is regulated as a consequence of odor exposure. Others have shown that increased intracellular cAMP results in selective internalization of the Tm form of apCAM because of phosphorylation of a sequence (PEST) in the intracellular domain (Bailey et al., 1997). As TmRNCAM contains a PEST sequence (Yoshihara et al., 1997), it is tempting to speculate that formation and/or maintenance of precise OR-specific connections is influenced by dynamic changes of surface-expressed TmRNCAM levels. Supporting this notion is the fact that the intensity of RNCAM immunoreactivity varies slightly between individual glomeruli (data not shown).

Axons of OSNs expressing a given OR take two routes that project to glomeruli located in either the medial or the lateral OB. An equal representation of OR-specific glomeruli and OR-zones in both the lateral and medial division suggests that each bulb has two symmetrical sensory maps (Nagao et al., 2000). Interestingly, the GpiRNCAM-specific phenotype is restricted to the lateral mirror map, while OSNs contributing to the medial mirror map was more sensitive to the effect of TmRNCAM. Our result thus suggests that the two mirror maps in each bulb are not formed or maintained with identical mechanisms. We do not find evidence for an uneven distribution of RNCAM mRNA splice variants or RNCAM immunoreactivity in glomeruli along dorsoventral, mediolateral and rostrocaudal aspects of OE or OB. Medially and laterally projecting P2 OSNs may be intrinsically different. Alternatively, differential sensitivity to the effects of the two RNCAM isoforms can be a consequence of interactions with signals having medial and lateral distribution. To address such issue it will be important to identify molecular cues that divide OSN projections in two mirror image maps, as well as proteins that directly interact with RNCAM.

Taken together, we have uncovered three important functional characteristics of RNCAM. First, RNCAM does not determine the division of OSN projections into Z1 and Z2-4, respectively. Second, normal regulated levels of RNCAM are important for accurate OR-specific axon segregation of Z2-4 OSNs. Finally, we identify specific activities of RNCAM splice variants that influence formation of precise topographic axon connections in the vicinity and distant relative to the correct target.

We thank Dr Peter Mombaerts for kindly providing P2-IRES-tau*lacZ* mice, Dr Frank Margolis for OMP antibody, Dr Bo Servenius for mouse genomic OMP clone and Dr A. Berghard for helpful comments on the manuscript. This work was supported by grants from the Swedish Natural Science Research Council (B5101-1250/2001), Petrus & Augusta Hedlund's Fund, the Swedish Society for Medical Research and the Magnus Bergvalls Fund.

REFERENCES

Alenius, M. and Bohm, S. (1997). Identification of a novel neural cell adhesion molecule-related gene with a potential role in selective axonal projection. *J. Biol. Chem.* **272**, 26083-26086.

Bailey, C. H., Kaang, B. K., Chen, M., Martin, K. C., Lim, C. S., Casadio, A. and Kandel, E. R. (1997). Mutation in the phosphorylation sites of MAP kinase blocks learning-related internalization of apCAM in Aplysia sensory neurons. *Neuron* **18**, 913-924.

Beckel-Mitchener, A. C., Miera, A., Keller, R. and Perrone-Bizzozero, N. I. (2002). Poly(A) Tail Length-dependent Stabilization of GAP-43 mRNA by the RNA-binding Protein HuD. *J. Biol. Chem.* **277**, 27996-28002.

Breitschopf, H., Suchanek, G., Gould, R. M., Colman, D. R. and Lassmann, H. (1992). In situ hybridization with digoxigenin-labeled probes: sensitive and reliable detection method applied to myelinating rat brain. *Acta Neuropathol.* **84**, 581-587.

Buck, L. and Axel, R. (1991). A novel multigene family may encode odorant receptors: a molecular basis for odor recognition. *Cell* **65**, 175-187.

Chess, A., Simon, I., Cedar, H. and Axel, R. (1994). Allelic inactivation regulates olfactory receptor gene expression. *Cell* **78**, 823-834.

Cloutier, J.-F., Giger, R., Koentges, G., Dulac, C., Kolodkin, A. L. and Ginty, G. G. (2002). Neuropilin-2 mediates axonal fasciculation, zonal segregation, but not axonal convergence, of primary accessory olfactory neurons. *Neuron* **33**, 877-892.

Conzelmann, S., Malun, D., Breer, H. and Strotmann, J. (2001). Brain targeting and glomerulus formation of two olfactory neuron populations expressing related receptor types. *Eur. J. Neurosci.* **14**, 1623-1632.

Danciger, E., Mettling, C., Vidal, M., Morris, R. and Margolis, F. (1998). Olfactory marker protein gene: its structure and olfactory neuron-specific expression in transgenic mice. *Proc. Natl. Acad. Sci. USA* **86**, 8565-8569.

Davis, B. J. (1991). NADPH-diaphorase activity in the olfactory system of the hamster and rat. *J. Comp. Neurol.* **314**, 493-511.

Davy, A., Gale, N. W., Murray, E. W., Klinghoffer, R. A., Soriano, P., Feuerstein, C. and Robbins, S. M. (1999). Compartmentalized signaling by GPI-anchored ephrin-A5 requires the Fyn tyrosine kinase to regulate cellular adhesion. *Genes Dev.* **13**, 3125-3135.

Dellacorte, C., Kalinoski, D. L., Huque, T., Wysocki, L. and Restrepo, D. (1995). NADPH diaphorase staining suggests localization of nitric oxide synthase within mature vertebrate olfactory neurons. *Neuroscience* **66**, 215-225.

Fambrough, D. and Goodman, C. S. (1996). The Drosophila beaten path gene encodes a novel secreted protein that regulates defasciculation at motor axon choice points. *Cell* **87**, 1049-1058.

Lin, D. M. and Ngai, J. (1999). Development of the vertebrate main olfactory system. *Curr. Opin. Neurobiol.* **9**, 74-78.

Malnic, B., Hirono, J., Sato, T. and Buck, L. B. (1999). Combinatorial receptor codes for odors. *Cell* **96**, 713-723.

Mombaerts, P., Wang, F., Dulac, C., Edmondson, J. and Axel, R. (1996). Visualizing an olfactory sensory map. *Cell* **87**, 675-686.

Nagao, H., Yoshihara, Y., Mitsui, S., Fujisawa, H. and Mori, K. (2000). Two mirror-image sensory maps with domain organization in the mouse main olfactory bulb. *NeuroReport* **11**, 3023-3027.

Norlin, E. M., Alenius, M., Gussing, F., Hagglund, M., Vedin, V. and Bohm, S. (2001). Evidence for gradients of gene expression correlating with zonal topography of the olfactory sensory map. *Mol. Cell. Neurosci.* **18**, 283-295.

Potter, S. M., Zheng, C., Koos, D. S., Feinstein, P., Fraser, S. E. and Mombaerts, P. (2001). Structure and emergence of specific olfactory glomeruli in the mouse. *J. Neurosci.* **21**, 9713-9723.

Ressler, K. J., Sullivan, S. L. and Buck, L. B. (1993). A zonal organization of odorant receptor gene expression in the olfactory epithelium. *Cell* **73**, 597-609.

Ressler, K. J., Sullivan, S. L. and Buck, L. B. (1994). Information coding in the olfactory system: evidence for a stereotyped and highly organized epitope map in the olfactory bulb. *Cell* **79**, 1245-1256.

Ross, J. (1995). mRNA stability in mammalian cells. *Microbiol. Rev.* **59**, 423-450.

Royal, S. J. and Key, B. (1999). Development of P2 olfactory glomeruli in P2-internal ribosome entry site-tau-LacZ transgenic mice. *J. Neurosci.* **19**, 9856-9864.

Sassoon, D. A., Garner, I. and Buckingham, M. (1988). Transcripts of α-cardiac and α-skeletal actins are early markers for myogenesis in the mouse embryo. *Development* **104**, 155-164.

Schaefer, M. L., Finger, T. E. and Restrepo, D. (2001). Variability of position of the P2 glomerulus within a map of the mouse olfactory bulb. *J. Comp. Neurol.* **436**, 351-362.

Servenius, B., Vernachio, J., Price, J., Andersson, L. C. and Peterson, P. A. (1994). Metastasizing neuroblastomas in mice transgenic for Simian virus 40 Large T (SV40T) under the olfactory marker protein gene promoter. *Cancer Res.* **54**, 5198-5205.

Simons, K. and Ikonen, E. (1997). Functional rafts in cell membranes. *Nature* **387**, 569-572.

Strotmann, J., Conzelmann, S., Beck, A., Feinstein, P., Breer, H. and Mombaerts, P. (2000). Local permutations in the glomerular array of the mouse olfactory bulb. *J. Neurosci.* **20**, 6927-6938.

Tsuboi, A., Yoshihara, S., Yamazaki, N., Kasai, H., Asai-Tsuboi, H., Komatsu, M., Serizawa, S., Ishii, T., Matsuda, Y., Nagawa, F. et al. (1999). Olfactory neurons expressing closely linked and homologous odorant receptor genes tend to project their axons to neighboring glomeruli on the olfactory bulb. *J. Neurosci.* **19**, 8409-8418.

Vassar, R., Chao, S. K., Sitcheran, R., Nunez, J. M., Vosshall, L. B. and Axel, R. (1994). Topographic organization of sensory projections to the olfactory bulb. *Cell* **79**, 981-992.

Vassar, R., Ngai, J. and Axel, R. (1993). Spatial segregation of odorant receptor expression in the mammalian olfactory epithelium. *Cell* **74**, 309-318.

Verhaagen, J., Oestreicher, A. B., Gispen, W. H. and Margolis, F. L. (1989). The expression of the growth associated protein B50/GAP43 in the olfactory system of neonatal and adult rats. *J. Neurosci.* **9**, 683-691.

Walsh, F. S. and Doherty, P. (1997). Neural cell adhesion molecules of the immunoglobulin superfamily: role in axon growth and guidance. *Annu. Rev. Cell Dev. Biol.* **13**, 425-456.

Wang, F., Nemes, A., Mendelsohn, M. and Axel, R. (1998). Odorant receptors govern the formation of a precise topographic map. *Cell* **93**, 47-60.

Winberg, M. L., Mitchell, K. J. and Goodman, C. S. (1998). Genetic analysis of the mechanisms controlling target selection:complementary and combinatorial functions of netrins, semaphorins, and IgCAMs. *Cell* **93**, 581-591.

Yoshihara, Y., Katoh, K. and Mori, K. (1993). Odor stimulation causes disappearance of R4B12 epitope on axonal surface molecule of olfactory sensory neurons. *Neuroscience* **53**, 101-110.

Yoshihara, Y., Kawasaki, M., Tamada, A., Fujita, H., Hayashi, H., Kagamiyama, H. and Mori, K. (1997). OCAM: A new member of the neural cell adhesion molecule family related to zone-to-zone projection of olfactory and vomeronasal axons. *J. Neurosci.* **17**, 5830-5842.

Yu, H. H., Huang, A. S. and Kolodkin, A. L. (2000). Semaphorin-1a acts in concert with the cell adhesion molecules fasciclin II and connectin to regulate axon fasciculation in Drosophila. *Genetics* **156**, 723-731.

Zheng, C., Feinstein, P., Bozza, T., Rodriguez, I. and Mombaerts, P. (2000). Peripheral olfactory projections are differentially affected in mice deficient in a cyclic nucleotide-gated channel subunit. *Neuron* **26**, 81-91.